Journal of Chromatography A, 1217 (2010) 7855–7863

Contents lists available at ScienceDirect

Journal of Chromatography A

journal homepage: www.elsevier.com/locate/chroma

Comparison of electrospray ionization, atmospheric pressure photoionization, and anion attachment atmospheric pressure photoionization for the analysis of hexabromocyclododecane enantiomers in environmental samples

Matthew S. Ross [a], Charles S. Wong [a,b,*]

[a] University of Alberta, Department of Chemistry, 11227 Saskatchewan Drive, Edmonton, Alberta T6G 2G2, Canada
[b] Environmental Studies Program and Department of Chemistry, Richardson College for the Environment, University of Winnipeg, Winnipeg, MB R3B 2E9, Canada

ARTICLE INFO

Article history:
Received 1 April 2010
Received in revised form
13 September 2010
Accepted 14 September 2010
Available online 14 October 2010

Keywords:
Atmospheric pressure photoionization
Hexabromocyclododecane
Matrix effects
Adduct formation

ABSTRACT

Anion attachment atmospheric pressure photoionization (AA-APPI) has been suggested as a means of expanding the range of compounds that may be analyzed by LC–MS, and has been found to enhance the ionization of some macromolecules (e.g., peptides, polymers) that were unable to be ionized by other techniques. In this study, AA-APPI was compared to APPI, using hexabromocyclododecane (HBCD) enantiomers as a model compound, to provide proof of principle of the use of AA-APPI for small molecule analysis. The use of AA-APPI, with 1,4-dibromobutane in toluene as a bromide source, offered increased sensitivity and lower limits of detection than APPI. Minimal matrix effects were found with AA-APPI in sediment extracts spiked with HBCD post-extraction, with less than a 6% enhancement in the ion signal. Furthermore, enantiomer fractions of HBCD enantiomers were racemic in spiked sediment extracts, in contrast to the more commonly used technique of electrospray ionization, for which matrix effects caused ion signal modification to cause non-racemic measurement artifacts. The use of AA-APPI offers a simple means of further extending the range of compounds ionizable by AA-APPI while maintaining minimal matrix effects.

1. Introduction

In recent years, liquid chromatography–mass spectrometry (LC–MS) has become increasingly popular for use in environmental analysis, and while a number of ionization techniques exist, electrospray ionization (ESI) remains the most widely used. However, while ESI is extremely sensitive for polar compounds, many environmental compounds are non-polar, and are therefore difficult to analyze using this technique. In 2000, atmospheric pressure photoionization (APPI) was developed as a complementary technique to ESI, and provides a means of ionizing low-polarity compounds [1]. For some analytes, APPI offers greater sensitivity [2,3] and larger dynamic ranges [4,5] than ESI. Furthermore, APPI may offer other advantages over ESI for environmental analyses. APPI ionization has been found to be less susceptible to matrix effects than ESI for a variety of analytes [4,6,7]. Matrix effects occur when the ionization efficiency of an analyte is either enhanced or suppressed, and is often attributed to matrix materials that co-elute with the analyte. This change in the analyte response can hamper quantification by leading to inaccurate and imprecise measurements of analyte concentration.

More recently, the use of anion attachment APPI (AA-APPI) has been suggested as a means of further expanding the range of compounds ionizable by APPI [8]. In general, the ionization of analytes by APPI relies on the presence of a photoionizable dopant, a low molecular weight compound with an ionization potential below that of the energies of the emitted photons. The dopant is introduced into the source, where it is photoionized to release a thermal electron. This, in turn, may initiate a series of gas phase reactions, subsequently yielding either a positively or negatively charged analyte ion [9]. In AA-APPI, analytes are ionized by the formation of a negatively charged adduct species within the source. The use of stable adducts to enhance the ionization of non-polar compounds in APPI, particularly large molecules such as peptides and polymers, has been demonstrated through the use of chlorinated solvents or chlorinated eluents [8,10,11]. However, to date this technique has not been shown to be applicable to small molecules, nor, to the best of our knowledge, do studies exist comparing the use of AA-APPI to other techniques, such as ESI or APPI.

Hexabromocyclododecane (HBCD) is a brominated flame retardant commonly added to consumer products, such as polystyrene

* Corresponding author at: Environmental Studies Program and Department of Chemistry, Richardson College for the Environment, University of Winnipeg, 515 Portage Ave., Winnipeg, MB R3B 2E9, Canada.
Tel.: +1 204 786 9335; fax: +1 204 775 2114.
E-mail address: wong.charles.shiu@alum.mit.edu (C.S. Wong).

0021-9673/$ – see front matter © 2010 Elsevier B.V. All rights reserved.
doi:10.1016/j.chroma.2010.09.083

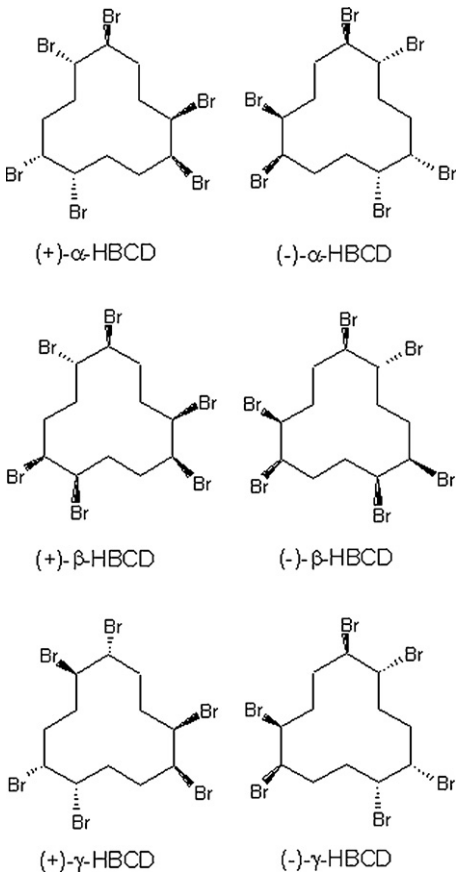

Fig. 1. Structures of major HBCD diastereomers and enantiomers.

foams and textiles, to reduce their flammability [12]. Within the last decade, increasing concentrations of HBCD have been found in air, sediment, biota, and human blood and milk [13]. Hexabromocyclododecane is present in the environment as a mixture of three major diastereomers: α, β, and γ (Fig. 1). Each diastereomer is chiral, and therefore each exists as a pair of enantiomers [14]. The chirality of a compound may have profound impacts on a compound's fate and behavior in the environment. For instance, individual enantiomers may vary in bioaccumulation, metabolism, and toxicology [15–19]. Therefore, the need exists to analyze chiral compounds on an enantiomer-specific basis in order to understand better the environmental fate of individual enantiomers. However, the accurate quantification of enantiomers is often hampered by matrix effects, as matrix effects may have a more detrimental effect on the quantification of enantiomers than on the sum mixture of enantiomers, as commonly measured by non-enantioselective chromatography as a single peak [20].

In this study, we compared the analytical characteristics and matrix effects of APPI and AA-APPI using HBCD as an environmentally relevant model compound. In doing so, we provide proof of principle evidence on the use of AA-APPI for the purposes of quantifying small molecules.

2. Experimental

2.1. Chemicals and reagents

Individual HBCD standards (α, β, and γ) were purchased from Accustandard (New Haven, CT, USA), all greater than 99% pure. Individual deuterated (d_{18}) HBCD isomers, of at least 98% chemical and isotopic purity, were purchased from Wellington Laboratories (Guelph, ON, Canada). HPLC grade methanol, acetonitrile, and toluene, as well as pesticide grade hexane and acetone were purchased from Fisher Scientific (Ottawa, ON, Canada), as was anhydrous sodium sulfate. Milli-Q water was obtained via a Millipore (Billerica, MA, USA) water filtration system. 1,4-Dibromobutane (99% purity) was purchased from VWR (Mississauga, ON, Canada). Silica gel (70–230 mesh) was purchased from Sigma–Aldrich (Oakville, ON, Canada). Certified reference material EC-5 (Lake Ontario sediment, certified for polyaromatic hydrocarbons, chlorobenzenes, and polychlorinated biphenyls) was obtained from Environment Canada.

2.2. Liquid chromatography/mass spectrometry

For all experiments, an Agilent 1100 HPLC system coupled to an Applied Biosystems QTrap 2000 (Foster City, CA) triple quadrupole mass spectrometer was used. Enantiomer separation was achieved on a Nucleodex β-PM enantioselective column (4.6 mm × 200 mm, 5 μm d_p, Macherey-Nagel, Bethlehem, PA) using an eluent of 49% acetonitrile/30% methanol/21% H_2O initially held for 2 min, then changed linearly to 59.5% acetonitrile/30% methanol/10.5% H_2O over 20 min at 500 μL min^{-1} [21]. This gradient was accomplished on a binary pump using 70:30 H_2O/methanol as the A solvent and 70:30 acetonitrile/methanol as the B solvent and changing the eluent composition from 30:70 A/B to 15:85 A/B over the course of the run [22]. Unless otherwise noted, an injection volume of 20 μL was used for all experiments. Chromatographic conditions were kept constant among source experiments.

Mass spectrometric experiments were carried out with a Photospray source (Applied Biosystems, Foster City, CA). Source parameters were optimized individually for all three sources in a similar manner. Optimization was done using a 1:1:1 mixture of all three native diastereomers (300 ng mL^{-1} each). An equal mixture of all three isomers was chosen in order not to place undue emphasis on one isomer over the others, as the mass spectral response may vary among isomers. This solution was introduced into the eluent flow via a tee connection at 20 μL min^{-1} using a syringe pump (Hamilton, Reno, NV). The eluent was flowed at 500 μL min^{-1}, and the composition was 77.5% A/22.5% B, which represents the midpoint in the gradient used for analysis. Optimization was carried out by systematically changing the user-adjustable source parameters to maximize the ion intensity of either the $[M-H]^-$ (APPI) or $[M+Br]^-$ (AA-APPI) ion (Table 1).

Unless otherwise noted, for all experiments and analyses, the carrier solvent or photoionization dopant was flowed into the source in conjunction with the auxiliary gas at 50 μL min^{-1} using either a syringe pump or a pneumatic delivery system [23]. For APPI experiments, toluene was used as the photoionization dopant.

2.3. Carrier solvent optimization

Prior to AA-APPI experiments and analyses, several experiments were carried out to determine the best source of bromide and the optimum carrier solvent (i.e., co-solvent being tested as a possible dopant) that would maximize the formation of the $[M+Br]^-$ ion. All experiments were carried out by injecting the analyte directly into the eluent flow, which was coupled to the mass spectrometer without any chromatographic column attached. For the first, 15 brominated aliphatic and alicyclic compounds of varying structures and degrees of bromination, were selected for screening due to their ready availability in our lab and their solubility in non-polar solvents. These compounds were characterized by their ability to fragment within the source to form bromide ions (m/z 79 and 81). This was done by injecting into the LC 1 μL of a 1% solution (v/v) of each compound in toluene. The LC eluent composition was held constant at 77.5% A/22.5% B at a rate of 500 μL min^{-1}. Full scan mass

Table 1
Optimized MS/MS variables. a.u. = arbitrary units as per instrumentation used.

Parameter	Units	AA-APPI $m/z = 722 \rightarrow 79$	APPI $m/z = 640 \rightarrow 79$
Dwell time (ms)	ms	100	100
Collision cell entrance potential	V	−32	−34
Curtain gas	a.u.	20	20
Collision gas	a.u.	10	5
Source temperature	°C	300	400
Sheath gas	a.u.	600	60
Turbo gas	a.u.	0	90
Ion spray voltage	V	−1100	−1200
Declustering potential	V	−14	−18
Entrance potential	V	−5	−5
Collision energy	eV	−52	−52
Collision cell exit potential	V	−2	−2

spectra were collected for each compound over the mass range of m/z 60–400 to determine the dominant ions formed through photoionization and to monitor the formation of m/z 79 and 81 ions. To determine the necessity of a photoionizable carrier solvent on the formation of the bromide ions, this experiment was carried out both with and without the addition of toluene introduced with the auxiliary gas at 50 μL min^{-1}.

We further screened the individual brominated compounds based on the formation of the $[M+Br]^-$ adduct, in order to determine whether or not the formation of the $[M+Br]^-$ adduct ion was based solely on the amount of Br^- formed from a particular compound, or whether other factors were involved. A 1:1:1 mixture of HBCD diastereomers (100 ng mL^{-1} final concentration) was spiked into solutions containing 1% (v/v) of individual brominated compounds in toluene. These solutions were injected (10 μL) into the eluent flow as described above, and the $[M+Br]^- \rightarrow Br^-$ transition was monitored by multiple reaction monitoring (MRM). No additional source of dopant was used during this experiment. Based on these two experiments, 1,4-dibromobutane (1,4-DBB) was chosen for use as the bromide source for the rest of the study.

From the first experiment, we found that the use of a photoionizable carrier solvent was necessary for the formation of bromide ions. Therefore, the carrier solvent was optimized based on its ability to function as a dopant (i.e. photoionize within the source), as the dopant has been found to affect the ionization of analytes in APPI [1,2,24]. The carrier solvent was optimized by injecting 5 μL of 1% (v/v) 1,4-DBB in either toluene, anisole, acetone, acetonitrile, hexane, heptane, or methanol and collecting full scan mass spectra from m/z 60–400. No additional dopant was used in these experiments. From the collected spectra, the abundance of bromide ions was compared between the different solvents. Next, the effects of the carrier solvent selection on the formation of HBCD adducts was investigated. A 1:1:1 mixture of HBCD diastereomers (1 μg mL^{-1} each) was added to the eluent flow via a tee connection, and 10 μL injections of 1% (v/v) 1,4-DBB in either toluene, anisole, acetone, acetonitrile, hexane, heptane, or methanol was injected into the LC with no additional source of dopant. The transitions from both the $[M+Br]^- \rightarrow Br^-$ and $[M-H]^- \rightarrow Br^-$ were monitored by MRM. The resultant peak areas were integrated using Analyst software, and compared among the solvents.

Finally, the influence of the brominated compound concentration on the formation of $[M+Br]^-$ was investigated. The formation of $[M+Br]^-$ was measured at 5 different concentrations of 1,4-DBB dissolved in toluene, ranging from 0.05% (v/v) to 2% (v/v). Each solution was introduced into the source in conjunction with the auxiliary gas at 50 μL min^{-1}. A 1:1:1 mixture of HBCD diastereomers (1 μg mL^{-1} each) was injected (10 μL) into the eluent flow and the formation of the $[M+Br]^-$ ion was monitored.

For calibration curve and matrix experiments, multiple reaction monitoring was used for analyte detection. For APPI experiments, the transitions from $[M-H]^- \rightarrow Br^-$ (m/z 640.6 → 78.9 and 80.9) were used, while for AA-APPI experiments, the transitions from $[M+Br]^- \rightarrow Br^-$ (m/z 722.6 → 78.9 and 80.9) were monitored. The d_{18}-labeled isomers were detected using analogous transitions. All results are reported as the parent ion to m/z 78.9 transition.

2.4. Determination of analytical variables

For the determination of analytical variables, a single set of standard solutions in methanol were made by solvent exchange of the initial stock standards from toluene to methanol and serial dilution of the initial stock standard to the desired concentrations. Each solution contained HBCD diastereomers in a 1:1:1 ratio, ranging in concentration from 1 to 1000 ng mL^{-1} for each diastereomer, and also contained 100 ng mL^{-1} of each d_{18}-labeled diastereomer. Analysis of each solution was done in triplicate on each source, producing a calibration curve for each individual enantiomer. From this, analytical variables such as linearity, limits of detection (LOD, mean signal of the blank + 3*standard deviation of the blank) and limits of quantification (LOQ, mean signal of the blank + 10*standard deviation of the blank) were determined on an enantiomer-specific basis.

2.5. Matrix effects experiments

The effect of co-extracted matrix materials from sediment samples on the analysis of HBCDs was compared among ionization methods. For this, a post-extraction addition method was done utilizing reference sediment as the matrix material. Using a 1:1 mixture of acetone:hexane, 3 g of CRM EC-5 was extracted overnight by Soxhlet extraction. Extracts were cleaned up by acidified silica gel chromatography, using 8 g of deactivated silica gel which had been 50% acidified by H_2SO_4 [25,26]. While a number of other extraction and cleanup procedures exist for HBCDs, this method was chosen as it likely retains much of the matrix material in the final extract. After cleanup, samples were divided into two aliquots and reduced in volume to 200 μL. The first aliquot was fortified with 40 ng of 1:1:1 mixture of HBCD diastereomers as well as a 40 ng of a 1:1:1 mixture of d_{18}-labeled HBCDs. The second aliquot remained unspiked. Extracts were then analyzed by LC–MS/MS on all three sources.

2.6. Data analysis

For flow injection analysis experiments, ion intensities and analyte peaks were integrated with Analyst software. Model-fitting software (PeakFit v.4.0, Systat, San Jose, CA) was used to determine the peak areas in chromatographic runs. This software was used due to the fact that some enantiomer peaks partially coeluted. Therefore, other methods of peak integration may lead to erroneous measurements of the enantiomer fractions [27]. For all analyses, peaks were fit to an exponentially modified Gaussian function, and

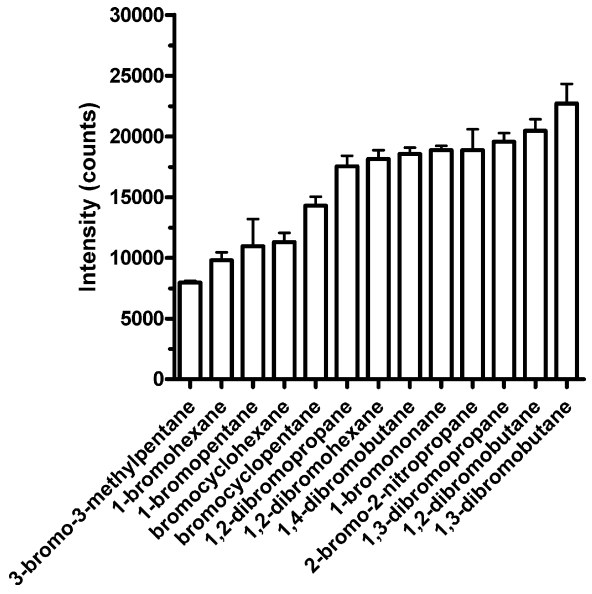

Fig. 2. The intensity of the $[M+Br]^- \rightarrow Br^-$ multiple reaction monitoring transition for the 15 screened brominated compounds (1% v/v) in toluene with 100 ng mL^{-1} of a 1:1:1 mixture of α-, β-, and γ-HBCD.

all peak widths were assumed to remain constant. These parameters were chosen as they were found to model best the peak shape in these experiments.

3. Results and discussion

3.1. Selection of AA-APPI bromine source

The use of stable adducts to enhance the ionization of non-polar compounds in APPI has previously been demonstrated, and was found to be particularly useful for large molecules such as peptides and polymers [8,10,11]. The formation of the adduct ion in these studies was achieved through the use of chlorinated eluents or solvents, both of which are incompatible with the reversed phase eluents needed to separate the HBCD enantiomers [22]. Therefore, to form the $[M+Br]^-$ ion, we introduced a source of bromide ions into the source in conjunction with a photoionizable carrier solvent, rather than adding brominated compounds or bromine salts into the eluent, as is typically done when generating adducts for ESI analyses.

To demonstrate the feasibility of using this technique, 15 brominated compounds were screened (Fig. 2), in order to determine their ability to fragment and form Br^- ions within the source. With the addition of toluene, all of the brominated compounds investigated could be fragmented to some degree. The dominant ion for all of the screened compounds was Br^-. For all of the compounds tested, there was at least an order of magnitude difference between amount of ions formed with and without toluene (Fig. SI1), indicating the necessity of a photoionizable solvent to facilitate the ionization of the brominated compounds. Additionally, all investigated compounds produced similar amounts of $[M+Br]^-$ adduct ions, and were within a 3-fold difference of each other (Fig. 2).

While selecting compounds to be screened, an attempt was made to choose compounds of varying structures and degrees of bromination. However, it was difficult to determine if there were any trends among the compounds in terms of the amount of bromide ions formed, based on the small sample size for this experiment. Furthermore, a comprehensive study of possible bromide sources was beyond the scope of this study. Due to the similarities among compounds, we chose to continue our experiments with 1,4-dibromobutane (1,4-DBB), as it was readily available in our lab. Based on other experiments using 1,4-DBB as a bromide source, there was a large excess of Br^- ions in the source during HBCD analyses, even at low concentrations of 1,4-DBB (data not shown). Given the similarities in bromide and $[M+Br]^-$ formation found among compounds, it is likely that most of the other brominated compounds investigated would have produced such an excess. This may indicate that the structure or choice of brominated compound may be of minor importance in determining the formation of the resulting $[M+Br]^-$ ion.

Table 2
Ionization potentials of dopants.

Compound	IP (eV)[a]
1,4-Dibromobutane	10.15
Toluene	8.83
Anisole	8.2
Acetone	9.7
Heptane	9.93
Hexane	10.13
Methanol	10.83

[a] From Ref. [30].

3.2. Selection of AA-APPI carrier solvent

Previous studies have found that the selection of the photoionization dopant has significant impacts on the analyte intensities in APPI [2,24,28,29], so we therefore investigated the influence of the photoionization of the carrier solvent on the formation of Br^- ions. This was done by monitoring the amount of Br^- ions formed from the photoionization of 1,4-DBB in various carrier solvents, encompassing a range of ionization potentials (IP, Table 2). In addition, anisole, toluene, and acetone have also been shown to impact the ionization of analytes in APPI [2,24,28,29].

From these experiments, we found that the fragmentation of 1,4-DBB and the formation of bromide ions in the source was not dependent simply on the presence of a photoionizable solvent, but was also dependent on the IP of carrier solvent in which the 1,4-DBB was dissolved. Toluene and anisole, which have the lowest IPs of the selected solvents, produced a significantly higher abundance of bromide ions than the other tested carrier solvents ($p < 0.05$). Following this observation, an inverse relationship was found between the amount of bromide ions produced and the ionization potential of the carrier solvent (Fig. 4A).

The need for a photoionizable dopant to be present in the source to facilitate the fragmentation of 1,4-DBB is due to the fact that the ionization potential of 1,4-DBB is greater than the energies of most of the emitted photons. The krypton lamp used in this study emits photons predominantly with energies of 10 eV, with a small proportion of 10.6 eV. At 10.15 eV, the IP of 1,4-DBB is greater than the predominant photon energy, making the direct photoionization of the 1,4-DBB unlikely. Rather, the 1,4-DBB was likely capturing an electron released from the photoionization of the carrier solvent, and subsequently dissociating to form bromide and a neutral fragment. Electron capture and dissociation of halogenated molecules has been observed previously [30], and has been suggested as necessary for facilitating the formation of adducts in APPI [10,11]. Similarly, a dopant (toluene) was necessary for the formation of adducts of larger molecules in APPI [11].

This proposed mechanism is consistent with our results. Of the carrier solvents investigated, only toluene, anisole, and acetone have ionization potentials less than the predominant photon energy produced by the krypton lamp used in this study (<10 eV). Therefore, these compounds are able to be ionized and release an electron into the source. However, bromide ions were formed even in the presence of heptane, hexane, and methanol, all solvents

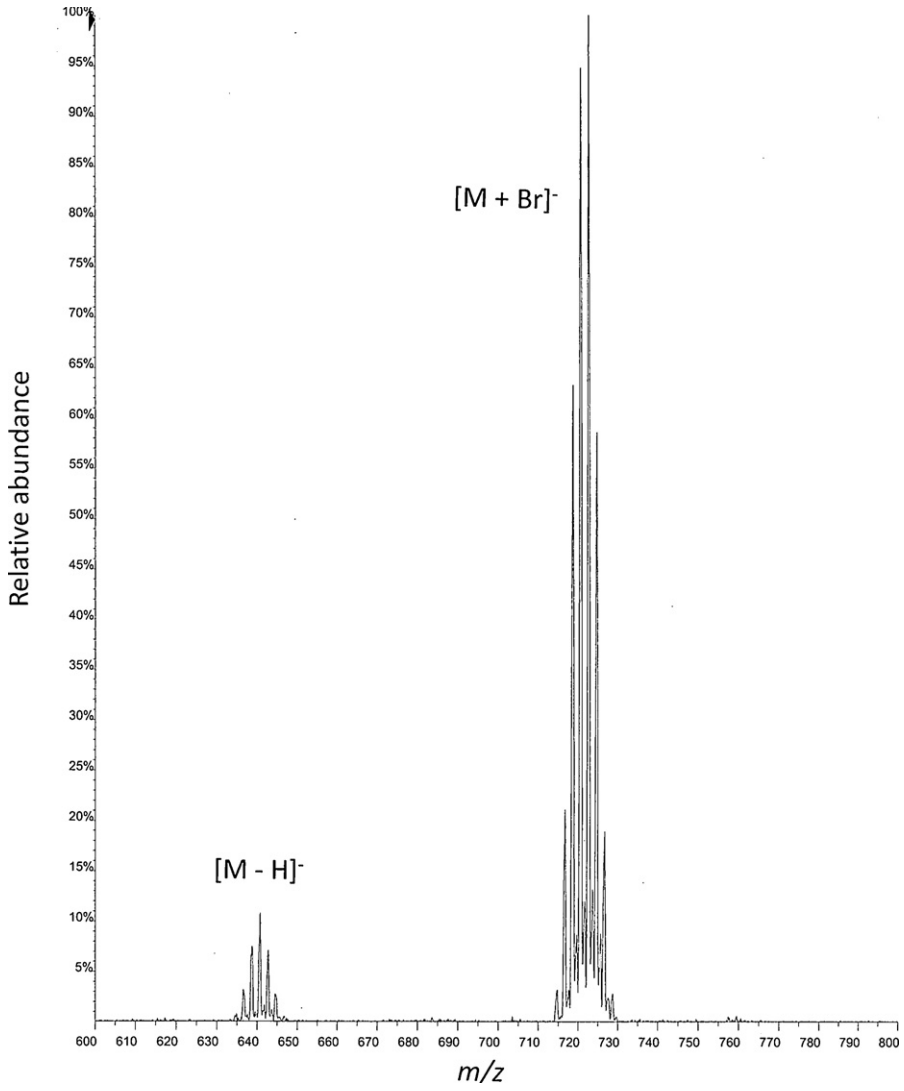

Fig. 3. APPI mass spectrum of HBCD diastereomers with 1% (v/v) 1,4-DBB in toluene as the carrier solvent, showing the formation of the $[M-H]^-$ (*m/z* 640.6) and $[M+Br]^-$ (*m/z* 722.6) ions.

with an IP very near or greater than 10 eV. As mentioned earlier, a small proportion of the photons produced may also have energies of 10.6 eV, which is greater than the IP of heptane or hexane. Therefore, some ionization of these compounds may be expected, and may explain the observed formation of bromide in the presence of these solvents. Methanol, however, has an IP of 10.8 eV. The bromide ions detected when using methanol as a carrier solvent may be attributed to the photoionization of 1,4-DBB itself, although this is unlikely given the lack of observation of a positive bromocyclobutane ion [31]. Alternatively, the formation of bromide ions in the presence of solvents with IPs greater than 10 eV may be due to the presence of electrons formed from the irradiation of the steel surfaces within the source [32]. Furthermore, an electron capture-dissociation mechanism is supported by our lack of finding of either an M^- or $[M-H]^-$ ion in the 1,4-DBB mass spectrum (data not shown), which would have indicated that other ionization processes, such as electron capture or proton transfer, were responsible for the ionization of 1,4-DBB.

Next, the effect of the carrier solvent on the formation of HBCD adducts was investigated. Through FIA experiments, we discovered that the $[M+Br]^-$ ion was predominantly formed, although a small percentage of $[M-H]^-$ ions were formed as well (Fig. 3). In order to maximize the formation of the $[M+Br]^-$ ion while minimizing the $[M-H]^-$ formation, we investigated how the ionization potential of the carrier solvent may influence the formation of both $[M+Br]^-$ and $[M-H]^-$ ions, using FIA and monitoring the $[M-H]^- \rightarrow Br^-$ and $[M+Br]^- \rightarrow Br^-$ transitions.

As with the previous experiment, there was a significant impact on the formation of $[M+Br]^-$ with the use of a photoionizable carrier solvent. The intensity of the $[M+Br]^- \rightarrow Br^-$ transition signal followed the same trend as seen for the formation of bromide, with toluene and anisole producing the highest signal for the $[M+Br]^- \rightarrow Br^-$ transition (Fig. 4B). This observation was not surprising, given that the amount of Br^- initially formed was itself dependent on the solvent used. However, there was little impact on the formation of $[M-H]^-$ ions by the various carrier solvents. There was no significant difference in the percentage of $[M-H]^-$ formed with the use of toluene, anisole or acetone, although all three of these solvents formed a significantly higher percentage of $[M-H]^-$ than did hexane. Moreover, with the exception of methanol, there was a general similarity in the percentage of $[M-H]^-$ formed (Fig. 4C). No differences were found in the intensity of $[M-H]^-$ ions formed with and without the addition of 1,4-DBB, in either toluene or anisole. Competition between the formation of the adduct ion and the deprotonated analyte ion has been observed previously [8,11]. The formation of either $[M-H]^-$ or $[M+Br]^-$ ions is a result of

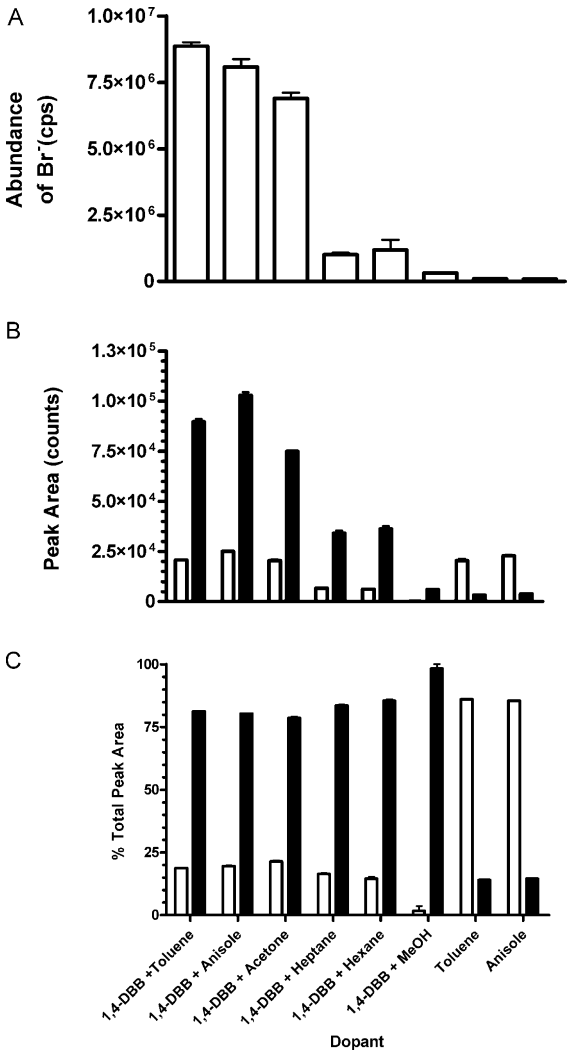

Fig. 4. Intensity of (A) bromide (m/z 79) and (B) peak areas of $[M-H]^-$ and $[M+Br]^-$ ions in various possible carrier solvents, and the (C) percentage of total peak area of each ion in the various carrier solvents. Total peak area equals the sum peak area of the $[M-H]^-$ and $[M+Br]^-$ produced by flow injection analysis. In (B) and (C), $[M-H]^-$ is represented by white bars and $[M+Br]^-$ is represented as black bars.

several competing reactions occurring within the source, although this data would indicate that the formation of $[M-H]^-$ occurs independently of the presence of bromide. Given the near-constant intensities of the $[M-H]^-$ ions, it may be that the formation of $[M-H]^-$ occurs quickly until a steady state is reached, at which point unreacted HBCD molecules may form brominated adducts. However, based on the results of this study, the mechanism and kinetics of these competing reactions is unknown, and warrants further investigation. Furthermore, if the formation of the $[M-H]^-$ ion could be suppressed, then an increase in the formation of the $[M+Br]^-$ ion would likely be seen. However, total suppression of the $[M-H]^-$ ion would only add an additional 20% maximum to the $[M+Br]^-$ ions formed (Fig. 4C).

Additionally, the formation of $[M-H]^-$ from the insource fragmentation of $[M+Br]^-$ and subsequent loss of HBr is unlikely. We investigated the collision induced dissociation of the adduct ion at various collisions energies ranging from 10 to 60 eV, and found that the only ion formed in these experiments was Br^- (data not shown). Therefore, any insource fragmentation would likely result in the formation of Br^- and neutral HBCD. Previous studies have found that the collision induced dissociation of chloride adducts of HBCD (formed during ESI) dissociated to form $[M-H]^-$. This was not observed in this study, likely due to the lower gas phase acidity of HBr compared to that of HCl [33,34].

Table 3
Linear regression results for calibration curves of individual enantiomers produced by APPI and AA-APPI.

Enantiomer	Calibration curve results			
	AA-APPI		APPI	
	Equation	R^2	Equation	R^2
(−)-α-HBCD	$y = 17.0x + 2.89$	0.998	$y = 6.78x + 4.69$	0.913
(+)-α-HBCD	$y = 17.4x + 3.12$	0.997	$y = 6.34x + 5.70$	0.927
(−)-β-HBCD	$y = 88.9x + 22.5$	0.998	$y = 22.9x + 13.7$	0.928
(+)-β-HBCD	$y = 88.1x + 23.0$	0.996	$y = 21.3x + 14.8$	0.939
(+)-γ-HBCD	$y = 91.7x + 23.7$	0.996	$y = 6.66x + 4.83$	0.947
(−)-γ-HBCD	$y = 91.4x + 18.4$	0.997	$y = 6.43x + 4.83$	0.946

Finally, the concentration of 1,4-DBB in toluene was optimized. The formation of $[M+Br]^-$ was measured at 5 different concentrations of 1,4-DBB, ranging from 0.05% (v/v) to 2% (v/v). At concentrations greater than 0.1%, there was no effect of concentration on $[M+Br]^-$ formation (Fig. SI2). These results indicate that at such concentrations, 1,4-DBB is well in excess of the amount needed to form adducts.

3.3. Comparison of analytical performance between APPI-based methods

To compare the analytical performance of APPI and AA-APPI, five-point calibration curves, encompassing a concentration range of 3 orders of magnitude (1–1000 ng mL^{-1} of each racemic diastereomer), were prepared and analyzed in triplicate with each method. Individual enantiomers were separated using an enantioselective LC–MS/MS method. Individual enantiomers were identified based on the elution order reported by Heeb et al. [14]. The peak area of each enantiomer was then fit to a linear regression line. From this, analytical parameters were determined on an enantiomer-specific basis.

For all comparisons, we used the $[M-H]^- \rightarrow 79$ and $[M+Br]^- \rightarrow 79$ transitions, as this is the transition most commonly used in the literature. Previous studies that have investigated the use of chloride adducts for the analysis of HBCDs by ESI have used the $[M+Cl]^- \rightarrow [M-H]^-$ transition for detection in MRM mode [35,36]. However, through the use of flow injection and infusion experiments, we found that the only daughter ion formed by the collision induced dissociation of the $[M+Br]^-$ ion was m/z 79 and 81.

For all enantiomers, the calibration curves produced by both methods were linear over the concentration ranges examined, with an average r^2 of 0.997 and 0.933 for the AA-APPI and APPI methods, respectively (Table 3). However, the average response factors (slope of the regression line) varied, depending on the diastereomer. Using AA-APPI, the γ- and β-HBCD isomers had equivalent response factors, which were more than 5-fold higher than that of the α isomer. Conversely, in APPI, the β isomer had a 3-fold higher response factor than did either the γ or α isomers, which were nearly equivalent. These differences in response factors between isomers and between methods translated into corresponding trends for LODs (Table 4), with the γ isomer having the lowest LOD using AA-APPI, which was 4.6-fold lower than the LOD using APPI. The LODs of the α and β isomer, however, were equivalent between the two methods. For both response factors and LODs, there were no differences between enantiomers of an individual isomer, regardless of method.

It should be noted that, while the LODs of the β and α isomers were similar between APPI and AA-APPI, the peak height response of the α, β, and γ isomers in AA-APPI were 3-, 4-, and 10-fold

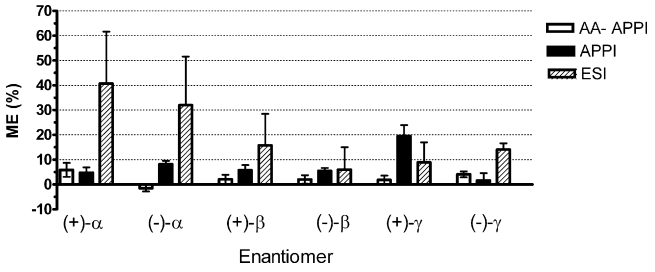

Fig. 5. Matrix effects on individual enantiomers in ESI, AA-APPI and APPI.

higher, respectively, than that of APPI. However, these enhancements in signal did not translate into equivalent decrease in LODs, due to the nearly 5-fold increase in background noise in AA-APPI. This increased noise was likely due to the addition of the 1,4-DBB.

The selective enhancement in the LODs of the γ isomer was interesting, as was the observation that the LODs of β and α isomers were only slightly or negligibly increased from APPI to AA-APPI. The enhancement of the γ isomer by AA-APPI may be linked to differences in the physical–chemical properties among diastereomers. For instance, Suzuki et al. found differences between the three diastereomers in terms of cavity diameter, dipole/dipole interactions, and charge density distributions [37]. The differences in charge density distribution were attributed to the higher response of β-HBCD in the formation of the $[M+Cl]^-$ adduct, and may play a role in the differences observed in this study. Furthermore, differences in the octanol–water partition coefficient (K_{ow}) among diastereomers have been reported, although their values have been debated. Hayward et al. found γ-HBCD to have the largest K_{ow} (and thus the most non-polar) [38], while Mariussen et al. [39] and Goss et al. [40] have found γ-HBCD to be the second most polar diastereomer, after α-HBCD. Due to the uncertainty in the physical properties of HBCD, it is difficult to speculate as to the cause of the increase in response of the γ isomer. However, the influence of chemical and physical properties on the ionization of an analyte by AA-APPI requires further investigation.

3.4. Matrix effects

The effects of co-extracted matrix material were evaluated in two ways. First, the extent of ion suppression or enhancement of individual enantiomers was quantified using a post-extraction addition technique. Sediment samples were extracted and spiked with a 1:1:1 mix of HBCDs prior to analysis. The same mixture of HBCDs was also spiked into methanol, and the resulting peak areas from the spiked sediment samples were compared to those from the methanolic solution. The percentage of ion suppression or enhancement was then quantified:

$$\text{ME\%} = \left(\frac{B}{A} - 1\right) \times 100 \quad (1)$$

where A is the peak area of the enantiomer in methanol, and B is the peak area of the enantiomer in the extracted sediment samples. If no suppression or enhancement of the response was occurring, the calculated percentage of matrix effects using the above formula would be zero, whereas percentages less than zero indicate ion suppression is occurring and values greater than zero indicate that the analyte signal is being enhanced.

The analyte signal was generally enhanced for all diastereomers (Fig. 5). Matrix effects in AA-APPI ranged from −1.5% for (−)-α-HBCD to 5.9% for (+)-α-HBCD, while the average matrix effects across all enantiomers was 2.2%. Similarly, the average matrix effects found in APPI ranged from 1.2% to 19.5%, although with the exception of (+)-γ-HBCD, all were less than a 10% enhancement. Both methods were very precise, with average RSDs of 3.5% and 4.3% for AA-APPI and APPI, respectively.

For all diastereomers, no differences in the matrix effects between the two enantiomers were observed. In addition, the effect of any HBCDs already present in the sediment extracts prior to spiking may be ruled out, as sediment extracts that remained unspiked, were analyzed and found to contain no detectable levels of HBCDs. Therefore, any signal enhancement must be attributed to matrix effects.

To compare these methods to the more commonly used techniques, all of the spiked sediment extracts and methanolic solutions were analyzed by ESI. Matrix effects in ESI ranged from 6.0% to 40.7% (Fig. 5), values which were similar to matrix effects found in food samples when using chloride adducts to quantify HBCDs by ESI [36]. It was clear that both APPI and AA-APPI showed considerable improvement over ESI in regards to matrix effects. The results from this study support many other studies which found an reduction in the matrix effects through the use of APPI [4,6,7].

Secondly, the effect of matrix effects on the quantification of enantiomers was investigated. This was done by determining the enantiomer fractions (EF) of HBCD enantiomers from the same extracts as described previously, and comparing them across the methods [41]:

$$EF = \frac{(+)}{(+)+(-)} \quad (2)$$

where (+) is the peak area of the (+) enantiomer, and (−) is the peak area of the (−) enantiomer. We assumed that the solution spiked into the sediment samples was racemic and that the mass spectral response factor between individual enantiomers is identical. Therefore, any deviations from a racemic EF of 0.5 were attributed to matrix effects.

Previous studies have reported that the EFs found using ESI deviated from 0.5, even in standard solutions containing racemic proportions of HBCD diastereomers. The non-racemic EFs have been attributed to differential effects of matrix between the two enantiomers or due to the differences in the ionization environment between the two enantiomers during the gradient elution [20,21]. The accurate measurement of EFs is essential, as it has been found that even small changes in the measured EF may lead to significant effects on the interpretation of enantiomer-specific data [27].

Using similar chromatography as previous studies, we found that AA-APPI and APPI produced nearly racemic EFs for all diastereomers (Table 5). Enantiomer fractions produced using AA-APPI were racemic for all diastereomers, ranging from 0.492 to 0.507. Using APPI, EFs deviated slightly from non-racemic and had larger variation than the EFs found using AA-APPI. This can likely be attributed to the low signal-to-noise ratio for these samples and the difficulty accurately fitting peaks under such conditions [24]. These results agree with the above post-addition spike data, with the lack of observed matrix effects subsequently leading to more accurate quantification of enantiomers in the samples.

Atmospheric pressure photoionization has previously been demonstrated to produce fewer matrix effects than ESI for the trace analysis of environmental contaminants in biological matrices [42]. While only sediment samples were used in the current study, we expect a similar lack of matrix effects for AA-APPI in biological matrices. How biological matrices may affect the measurement of the enantiomer distribution, however, must be investigated further.

It should be noted that for HBCDs, ESI produced a 5–25-fold lower LOD than either APPI or AA-APPI (data not shown). The ESI LODs were consistent with previous results [20–22]. The differences in ionization efficiency of an analyte among the different ionization methods will be based on the physical–chemical prop-

Table 4
Analytical performance characteristics of AA-APPI and APPI.

Enantiomer	Limit of detection (LOD)				Limit of quantification (LOQ)			
	AA-APPI		APPI		AA-APPI		APPI	
	Mass (pg)	Standard Dev.	Mass (pg)	Standard Dev.	Mass (pg)	Standard Dev.	Mass (pg)	Standard Dev.
(−)-α-HBCD	459	6	370	101	1380	19	1180	323
(+)-α-HBCD	449	6	391	96	1350	19	1250	308
(−)-β-HBCD	88	2	109	28	264	5	348	88
(+)-β-HBCD	89	2	116	27	266	5	371	86
(+)-γ-HBCD	85	2	369	81	256	5	1180	259
(−)-γ-HBCD	104	2	480	127	311	5	1540	407

Table 5
Enantiomer fractions of HBCD diastereomers in post-extraction spiked certified reference material EC-5 sediment samples.

	AA-APPI		APPI		ESI	
	EF	Standard Dev.	EF	Standard Dev	EF	Standard Dev
α-HBCD	0.507	0.013	0.510	0.017	0.506	0.009
β-HBCD	0.503	0.005	0.516	0.013	0.509	0.025
γ-HBCD	0.492	0.003	0.521	0.016	0.489	0.036

erties of the analyte. Despite the decrease in sensitivity compared to ESI that is seen here for HBCDs, analysis by AA-APPI and APPI has been shown be advantageous for some analytes [2–5]. Furthermore, the ability to reduce matrix effects and yield more accurate results may offset the reduction in sensitivity for other analytes. While the use of a mass-labeled internal standard may compensate for any matrix effects and lead to more accurate quantification of the EF [20], for many compounds, chiral or otherwise, mass-labeled versions are unavailable. For these analytes, we suggest that use of APPI or AA-APPI may lead to more accurate quantification of such analytes.

4. Conclusions

Through the inclusion of brominated compounds into the dopant flow, we have demonstrated a novel method for the formation of adduct species by APPI and the viability of AA-APPI for the analysis of small molecules, using HBCD as a model compound. Lower limits of detection were produced through the use of AA-APPI compared to APPI, particularly for the γ-HBCD isomer. Moreover, AA-APPI was relatively unaffected by matrix effects from extracted sediment, similar to APPI, and considerably less so than ESI. While matrix effects may be compensated for using isotopically labeled standards, as is the case for HBCDs, there is a lack of such standards available for many environmentally relevant compounds. Therefore, the use of AA-APPI and APPI is an attractive technique to quantify enantiomers in environmental samples for those compounds for which an isotopically labeled standard is unavailable.

Acknowledgements

This work was funded by the Natural Sciences and Engineering Research Council of Canada, and the Canada Research Chairs program.

Appendix A. Supplementary data

Supplementary data associated with this article can be found, in the online version, at doi:10.1016/j.chroma.2010.09.083.

References

[1] D.B. Robb, T.R. Covey, A.P. Bruins, Anal. Chem. 72 (2000) 3653.
[2] N. Itoh, Y. Aoyagi, T. Yarita, J. Chromatogr. A 1131 (2006) 285.
[3] A. Riu, D. Zalko, L. Debrauwer, Rapid Commun. Mass Spectrom. 20 (2006) 2133.
[4] H.B. Theron, M.J. van der Merwe, K.J. Swart, J.H. van der Westhuizen, Rapid Commun. Mass Spectrom. 21 (2007) 1680.
[5] K.S. Hakala, L. Laitinen, A.M. Kaukonen, J. Hirvonen, R. Kostiainen, T. Kotiaho, Anal. Chem. 75 (2003) 5969.
[6] M. Takino, T. Tanaka, K. Yamaguchi, T. Nakahara, Food Addit. Contam. 21 (2004) 76.
[7] I. Marchi, S. Rudaz, M. Selman, J.-L. Veuthey, J. Chromatogr. B 845 (2007) 244.
[8] L.G. Song, A.D. Wellman, H.F. Yao, J.E. Bartmess, J. Am. Soc. Mass Spectrom. 18 (2007) 1789.
[9] T.J. Kauppila, T. Kotiaho, R. Kostiainen, A.P. Bruins, J. Am. Soc. Mass Spectrom. 15 (2004) 203.
[10] A. Delobel, S. Roy, D. Touboul, K. Gaudin, D.P. Germain, A. Baillet, F. Brion, P. Prognon, P. Chaminade, O. Laprevote, J. Mass Spectrom. 41 (2006) 50.
[11] S. Kéki, J. Török, L. Nagy, M. Zsuga, J. Am. Soc. Mass Spectrom. 19 (2008) 656.
[12] M. Alaee, P. Arias, A. Sjödin, Å. Bergman, Environ. Int. 29 (2003) 683.
[13] A. Covaci, A.C. Gerecke, R.J. Law, S. Voorspoels, M. Kohler, N.V. Heeb, H. Leslie, C.R. Allchin, J. de Boer, Environ. Sci. Technol. 40 (2006) 3679.
[14] N.V. Heeb, W.B. Schweizer, M. Kohler, A.C. Gerecke, Chemosphere 61 (2005) 65.
[15] S.W. Smith, Toxicol. Sci. 110 (2009) 4.
[16] N.A. Warner, J.W. Martin, C.S. Wong, Environ. Sci. Technol. 43 (2009) 114.
[17] A.H. Buckman, C.S. Wong, E.A. Chow, S.B. Brown, K.R. Solomon, A.T. Fisk, Aquat. Toxicol. 78 (2006) 176.
[18] C.S. Wong, S.A. Mabury, D.M. Whittle, S.M. Backus, C. Teixeira, D.S. DeVault, C.R. Bronte, D.C.G. Muir, Environ. Sci. Technol. 38 (2004) 84.
[19] K. Wiberg, R.J. Letcher, C.D. Sandau, R.J. Norstrom, M. Tysklind, T.F. Bidleman, Environ. Sci. Technol. 34 (2000) 2668.
[20] C.H. Marvin, G. MacInnis, M. Alaee, G. Arsenault, G.T. Tomy, Rapid Commun. Mass Spectrom. 21 (2007) 1925.
[21] K. Janák, A. Covaci, S. Voorspoels, G. Becher, Environ. Sci. Technol. 39 (2005) 1987.
[22] N.G. Dodder, A.M. Peck, J.R. Kucklick, L.C. Sander, J. Chromatogr. A 1135 (2006) 36.
[23] R.D. McCulloch, D.B. Robb, M.W. Blades, Rapid Commun. Mass Spectrom. 22 (2008) 3549.
[24] T.J. Kauppila, R. Kostiainen, A.P. Bruins, Rapid Commun. Mass Spectrom. 18 (2004) 808.
[25] C.H. Marvin, G.T. Tomy, M. Alaee, G. MacInnis, Chemosphere 64 (2006) 268.
[26] J. de Boer, C. Allchin, R. Law, B. Zegers, J.P. Boon, Trends Anal. Chem. 20 (2001) 591.
[27] B.J. Asher, L.A. D'Agostino, J.D. Way, C.S. Wong, J.J. Harynuk, Chemosphere 75 (2009) 1042.
[28] D.R. Smith, D.B. Robb, M.W. Blades, J. Am. Soc. Mass Spectrom. 20 (2009) 73.
[29] D.B. Robb, D.R. Smith, M.W. Blades, J. Am. Soc. Mass Spectrom. 19 (2008) 955.
[30] T. Sunagawa, H. Shimamori, Int. J. Mass Spectrom. 205 (2001) 285.
[31] R.H. Staley, R.D. Wieting, J.L. Beauchamp, J. Am. Chem. Soc. 99 (1977) 5964.
[32] E. Basso, E. Marotta, R. Sergalia, M. Tubaro, P. Traldi, J. Mass Spectrom. 38 (2003) 1113.
[33] J.H. Zhu, R.B. Cole, J. Am. Soc. Mass Spectrom. 11 (2000) 932.

[34] R.B. Cole, J.H. Zhu, Rapid Commun. Mass Spectrom. 13 (1999) 607.
[35] P. Galindo-Iranzo, J.E. Quintanilla-López, R. Lebron-Aguilar, B. Gómara, J. Chromatogr. A 1216 (2009) 3919.
[36] B. Gómara, R. Lébron-Aguilar, J.E. Quintanilla-López, M.J. González, Anal. Chim. Acta 605 (2007) 53.
[37] S. Suzuki, A. Hasegawa, Anal. Sci. 22 (2006) 469.
[38] S.J. Hayward, Y.D. Lei, F. Wania, Environ. Toxicol. Chem. 25 (2006) 2018.
[39] E. Mariussen, M. Haukås, H.P.H. Arp, K.-U. Goss, A. Borgen, T.M. Sandanger, J. Chromatogr. A 1217 (2010) 1441.
[40] K.-U. Goss, H.P.H. Arp, G. Bronner, C. Niederer, J. Chem. Eng. Data 53 (2008) 750.
[41] T. Harner, K. Wiberg, R. Norstrom, Environ. Sci. Technol. 34 (2000) 218.
[42] S. Chu, R.J. Letcher, J. Chromatogr. A 1215 (2008) 92.